Computation of Unstable Binodals Not Requiring Concentration Derivatives of the Gibbs Energy

R. Horst

Johannes Gutenberg-Universität, Institut für Physikalische Chemie, Jakob-Welder-Weg 13, D-55099 Mainz, Germany

Received: February 6, 1997; In Final Form: July 9, 1997

The equilibrium of three liquid phases in a binary mixture implies the existence of tie lines and binodals that are different from the normal experimentally observable ones. First of all, there are the metastable extensions of the binodal built up by S/S tie lines. These S/S tie lines fulfill the equilibrium condition of the minimum of the Gibbs energy of the entire two-phase system. Both coexisting phases are located within the meta-(stable) region. There are two additional types of tie lines: U/U (maximum of the Gibbs energy; both end points within the unstable area) and U/S tie lines (saddle point; one end point within the (meta)stable, the other within the unstable region). All types of tie lines fulfill the condition that the chemical potentials of each component have to be equal in the two phases given by the end points of the tie line. It is shown how all these tie lines build up the binodal and which rules they have to obey. A method for the calculation of all types of tie lines is presented that requires only the knowledge of the Gibbs energy of mixing; there is no need to calculate the chemical potentials. The method is applied to a Sanchez−Lacombe lattice fluid, and a polymer solution described by an extended Flory−Huggins model accounting for nonpolar and polar interactions.

Introduction

The occurrence of three-phase equilibria in binary mixtures is connected with unstable binodals and the theory of critical points, which was developed by Korteweg.[1] van der Waals[2] comprehensively described the phase diagrams with three-phase equilibria and the corresponding phenomena, as well as Tompa.[3]

The aim of this paper is the investigation of the binodal, i.e., the curve in the temperature−composition plane given by the end points of the tie lines. In a phase diagram with an unstable critical point there exist unstable binodals that were shown for the case of equilibria of exclusively liquid phases in polymeric systems by Šolc and Koningsveld.[4,5] These unstable binodals may also be possible without an unstable critical point, when there are two ranges of instability for a given temperature.[5]

The method[6] of calculating phase diagrams only on the basis of the energy of mixing without the requirement of evaluating its derivatives with respect to the composition variables will be extended to these types. In some exemplary phase diagrams the application of the present method will be demonstrated, the Gibbs energy being described by lattice theories neglecting as well as accounting for the effect of compressibility and polar interactions.

Interrelation of the Gibbs Energy and the Tie Lines

The normally applied coexistence condition is the equality of the chemical potentials $\mu_i^{(P)}$ of each substance (subscript) in all coexisting phases (superscript, written in parentheses to prevent confusion with exponents). For each tie-line the number of coexisting phases equals two. In a plot of G, the Gibbs energy per unit volume, or of G, the Gibbs energy per mol of lattice sites (with a given molar volume per lattice site V_s), versus the volume fraction φ of one of the components, the solutions to the coexistence condition are the contact points of the double tangents to $G(\varphi)$, giving the compositions of the coexisting phases. This is demonstrated in Figure 1 for a thermodynamic situation near a three-phase equilibrium. All six possible double tangents are drawn in Figure 1.

The decisive quantity determining the tie lines is G^{tp}, the Gibbs energy of the overall two-phase system, or the corresponding Gibbs energy of mixing ΔG^{tp}. In Figure 2 it can be seen that G^{tp} is not a minimum for all of the tie lines. One refers to an absolute minimum; here the phase-separated system is stable. For the given overall composition of 0.275 (indicated in Figure 1 by the arrow) only the left stable two-phase system is possible, since the value of φ_1^{tp} must be between those of the two phases. One tie line corresponds to a local minimum of G^{tp} (metastable two-phase system). Both end points of these three tie lines, the nodes, are located within the meta(stable) region of the phase diagram and therefore these tie lines are called **S/S tie lines**. The term "(meta)stable" is an abbreviation for "stable or metastable".

The full square in Figure 2 indicates a local maximum of G^{tp}. This maximum refers to the uppermost double tangent in Figure 1. The corresponding tie line is called **U/U tie line**. Both nodes are located within the unstable region. The two remaining tie lines are named **U/S tie lines**. One of their nodes is within the unstable region, the other within the (meta)stable area of the phase diagram. They correspond to saddle points of G^{tp}, not to extrema. Since G^{tp} is not a minimum for these two types of tie lines, the phase-separated system is not at equilibrium; it is unstable.

Calculation of Tie Lines

The mathematical description of the equality of the chemical potentials reads

S1089-5647(97)00480-X CCC: $15.00
Published on Web 04/04/1998

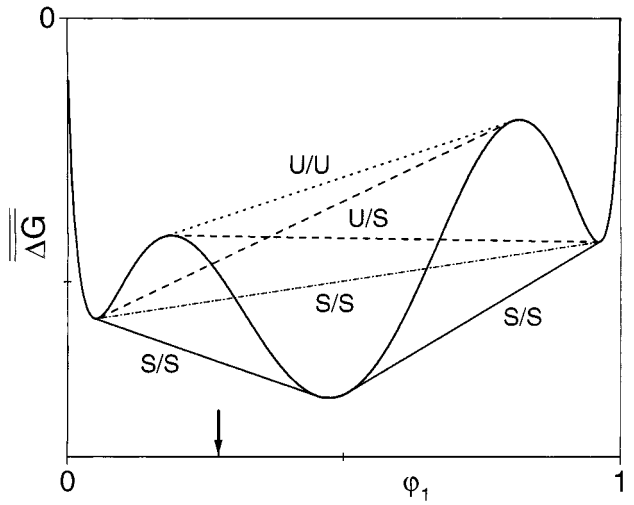

Figure 1. Scheme of the Gibbs energy of mixing per lattice site, ΔG, as a function of the volume fraction of component 1, φ_1, demonstrating the position of tie lines. The arrow indicates the overall composition for Figure 2.

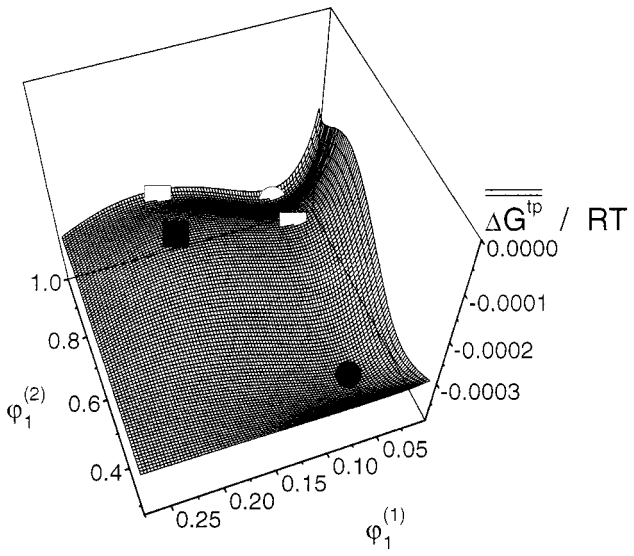

Figure 2. Dependence of the Gibbs energy of mixing of the entire two-phase system on the composition of the two phases at an overall volume fraction of $\varphi_1^{tp} = 0.275$. Full circle: absolute minimum, open circle: local minimum, full square: local maximum, open squares: saddle points.

$$\mu_i^{(1)} = \mu_i^{(2)} \qquad i = 1, 2 \tag{1}$$

Defining the conditions with G requires the Gibbs energy of mixing of the overall two-phase system per mol of lattice sites, ΔG, which is given by the values for the two phases by

$$\overline{\overline{\Delta G^{tp}}} = \sum_{j=1}^{2} \psi^{(j)} \overline{\overline{\Delta G^{(j)}}} \qquad \varphi_i^{tp} = \sum_{j=1}^{2} \psi^{(j)} \varphi_i^{(j)} \qquad i = 1, 2 \tag{2}$$

where $\psi^{(j)}$ is the part of the total volume occupied by phase j. The most fundamental equilibrium condition is the minimum of G^{tp} as a function of the compositions of the two phases for a given overall composition (S/S tie lines):

$$\overline{\overline{\Delta G^{tp}}}(\varphi_1^{(1)}, \varphi_1^{(2)}) = \min \tag{3}$$

The condition for the U/U tie lines reads

$$\overline{\overline{\Delta G^{tp}}}(\varphi_2^{(1)}, \varphi_2^{(2)}) = \max \tag{4}$$

The calculation of the U/S tie lines, i.e., finding the saddle point of G^{tp}, is relatively difficult, while the determination of minima or maxima is a very common mathematical iteration procedure.

The basis for the considerations is the Taylor expansion for a function f depending on one variable x:

$$f(x + \delta) = f(x) + f'(x)\,\delta + \ldots \tag{5}$$

Evidently, the difference between $f(x)$ for two very close x values is proportional to the first derivative $f'(x)$. From this it follows that the function $g(x)$

$$g(x) = [f(x + \delta) - f(x)]^2 \tag{6}$$

exhibits a minimum for all x values where the derivative of $f(x)$ equals zero. The minimum approaches zero for infinitely small δ values. Since G^{tp} is a function of two variables, $\varphi_1(1)$ and $\varphi_1(2)$, one has to take into consideration a sufficient number of points m around $(\varphi_1(1),\varphi_1(2))$ within the distance d in the process of numerical search for the minimum. In the present calculation $d = 10^{-6}$ and $m = 40$. This leads to the following condition for tie lines:

$$\sum_{i=1}^{m}\left[\overline{\overline{\Delta G^{tp}}}\left(\varphi_1^{(1)} + d\sin\frac{2\pi i}{m}, \varphi_1^{(2)} + d\cos\frac{2\pi i}{m}\right) - \overline{\overline{\Delta G^{tp}}}(\varphi_1^{(1)}, \varphi_1^{(2)})\right]^2 = \min \tag{7}$$

Figure 3 shows schematically the differences over which the summation in eq 7 proceeds as small lines for the five tie lines possible at the overall composition of 0.275. For the sake of better visibility, the value of d is chosen very big and the differences (vertical bars) are enlarged. They are large for points that do not correspond to double tangents (gray circle), whereas they become very small for each tie line. Equation 7 is the counterpart within the present concept to the condition of equality of chemical potentials (eq 1). Therefore it has the same disadvantage: it is also fulfilled for the trivial solution where the two phases are identical (cf. Figure 3, gray square, an overall composition close to this point). Dividing by the tie-line length prevents the trivial solution.[7] Near this solution the denominator, i.e., the length of the tie line, becomes zero causing the whole function to diverge. It turns out to be even better to divide by the tie-line length to the fourth.[7] The final condition reads

$$\sum_{i=1}^{m}\left[\overline{\overline{\Delta G^{tp}}}\left(\varphi_1^{(1)} + d\sin\frac{2\pi i}{m}, \varphi_1^{(2)} + d\cos\frac{2\pi i}{m}\right) - \overline{\overline{\Delta G^{tp}}}(\varphi_1^{(1)}, \varphi_1^{(2)})\right]^2 / (\varphi_1^{(1)} - \varphi_1^{(2)})^4 = \min \tag{8}$$

This is the condition that can be used to calculate all types of tie lines. Tie lines fulfilling only the condition of eq 7 but not those of eq 3 or eq 4 are the U/S tie lines.

Examples

Sanchez−Lacombe. The Sanchez−Lacombe lattice fluid[8] accounts for the free volume by introducing empty lattice sites. The quantities in eq 2 are replaced by quantities that refer to the close-packed state: ϕ_i, the close-packed volume fraction, and $\xi^{(j)}$ the part of the close-packed volume occupied by phase

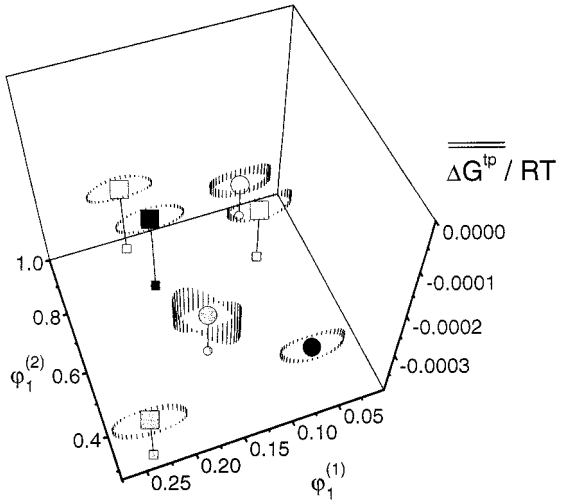

Figure 3. Scheme demonstrating the calculation of tie lines according to eq 7. Black and white symbols as in Figure 2, gray square: close to the trivial solution (both phases identical), gray circle: point not satisfying eq 7. The lines are the differences over which the summation in eq 7 is carried out.

j. (*g* is the Gibbs energy per segment, which will be described later.)

$$g^{\mathrm{tp}} = \sum_{j=1}^{2} \xi^{(j)} g^{(j)} \qquad \phi_i^{\mathrm{tp}} = \sum_{j=1}^{2} \xi^{(j)} \phi_i^{(j)} \qquad i = 1, 2 \quad (9)$$

Each pure component is characterized by the three scale factors T^* (characteristic temperature), P^* (characteristic pressure), and ρ^* (close-packed mass density). The total interaction energy per mer is given by

$$\epsilon^* = kT^* = P^* v^* \quad (10)$$

where v^* is the volume of a lattice site. r, the number of mers per molecule, can be evaluated by

$$r = M/\rho^* v^* N_{\mathrm{L}} \quad (11)$$

with M the molar mass and N_{L} Avogadro's constant or the Loschmidt number. The reduced pressure, temperature, volume, and density are given by

$$\tilde{X} = X/X^* \qquad X = P, v, T, \rho \quad (12)$$

where

$$\tilde{v} = 1/\tilde{\rho} \quad (13)$$

By fitting the equation of state

$$\tilde{\rho}^2 + \tilde{P} + \tilde{T}[\ln(1 - \tilde{\rho}) + (1 - (1/\mathrm{r}))\tilde{\rho}] = 0 \quad (14)$$

to density data for different temperatures and pressures the scale parameters can be determined.

In a mixture of two components v^*, the average close-packed volume of a mer, is identical for both components. The composition can be described by the close-packed mer or volume fraction ϕ_{i}, by the mole fraction

$$x_1 = \phi_1 \Big/ \left(\phi_1 + \phi_2 \frac{r_1^0 v_1^*}{r_2^0 v_2^*} \right) \quad (15)$$

where r_i is the number of mers per molecule of component *i* in the mixture, the superscript 0 indicates the value of $\mathrm{r_i}$ in the pure component *i*, or by the mass fraction:

$$m_1 = \frac{x_1 M_1}{x_1 M_1 + x_2 M_2} \quad (16)$$

The close-packed density of the mixture is interrelated with the values of the pure fluids by

$$\rho^* = 1 \Big/ \left(\frac{m_1}{\rho_1^*} + \frac{m_2}{\rho_2^*} \right) \quad (17)$$

and the average number of mers per molecule by

$$r = x_1 r_1^0 + x_2 r_2^0 \quad (18)$$

With

$$\phi_1^0 = r_1^0 x_1 / r \quad (19)$$

v^*,the average close-packed volume of a mer in the mixture, can be calculated as

$$v^* = \phi_1^0 v_1^* + \phi_2^0 v_2^* \quad (20)$$

The number of mers per molecule *i* in the mixture and the pure state are related by

$$r_i = r_i^0 v_i^* / v^* \quad (21)$$

For the present calculation parameters for the blend PVME/deuterated PS (see Table 1) are taken from ref 9, Figure 3a, to model the phase diagram as realistically as possible. In the present publication the interaction energy for the 1−2 interaction is slightly changed by adding a term quadratic in ϕ_2 to generate unstable critical points:

$$\epsilon^*_{12} = (\epsilon^*_{12})_0 + \Delta\epsilon \phi_2^{\,2} \quad (22)$$

The interaction energy of the mixture is

$$\epsilon^* = \phi_1^{\,2} \epsilon^*_{11} + \phi_2^{\,2} \epsilon^*_{22} + 2\phi_1 \phi_2 \epsilon^*_{12} \quad (23)$$

With eq 10 one can calculate T^* and P^* of the mixture. The Gibbs energy per mer (*rN* is the number of mers), is given by

$$g = \frac{G}{rN} = \epsilon^* \left\{ -\tilde{\rho} + \tilde{P}\tilde{v} \left[(1 - \tilde{\rho}) \ln(1 - \tilde{\rho}) + \frac{\tilde{\rho}}{\mathrm{r}} \ln \tilde{\rho} \right] + \tilde{T} \left[\frac{\phi_1}{r_1} \ln \phi_1 + \frac{\phi_2}{r_2} \ln \phi_2 \right] \right\} \quad (24)$$

Figure 4 shows the spinodals calculated with the parameters given in Table 1. For $\Delta\epsilon = 0$ the curve is identical to Figure 3a of ref 9. With decreasing $\Delta\epsilon$ the miscibility at low ϕ_1 values is decreased and a new minimum and maximum, i.e., a pair of new critical points, develop. Figure 5 gives the section of Figure

TABLE 1: Equation of State Parameters, Molar Masses, and Interaction Energy, Taken from Ref 9 for the System PVME/*d*-PS

	component 1	component 2
T^*/K	657	735
P^*/atm (1 atm = 101 325 Pa)	3580	3530
ρ^*/(kg/m^3)	1100	1190
M/(kg/mol)	389	230
$(\epsilon^*_{12})_0/k$/K	696.678	

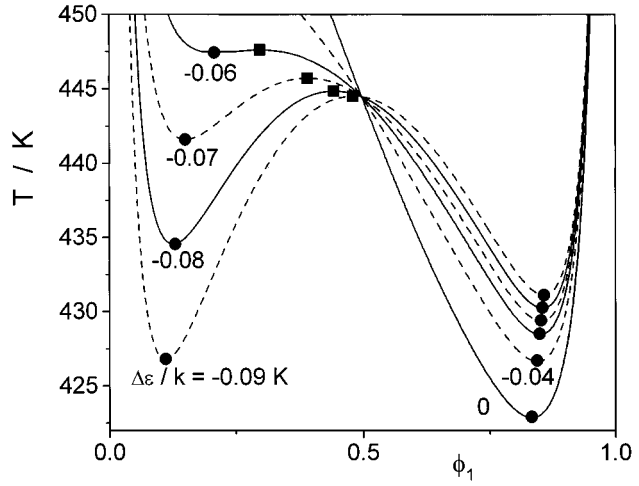

Figure 4. Spinodals calculated with the set of parameters given in Table 1 and the $\Delta\epsilon$ values given in the graph. Full circles: stable critical points, full squares: unstable critical points.

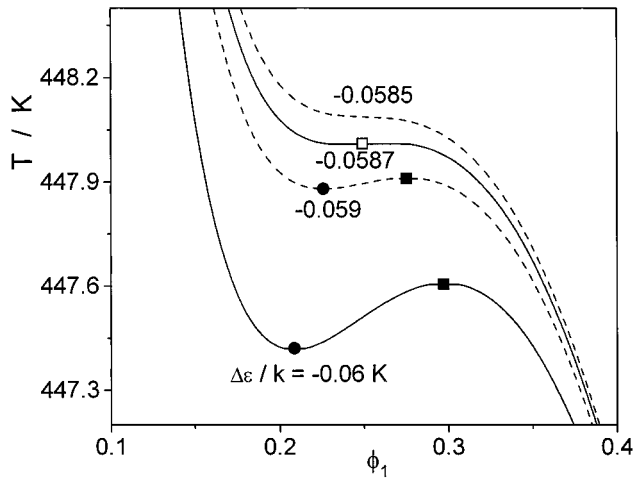

Figure 5. Spinodals for $\Delta\epsilon$ values close to the one causing the appearance of a heterogeneous double critical point. Open square: heterogeneous double critical point, other symbols as in Figure 4.

4 where the first new minimum and maximum occur. At $\Delta\epsilon/k = -0.0587$ the spinodal exhibits a shoulder with a horizontal tangent, and the point of inflection is the location of a double critical point. At somewhat smaller values the shoulder develops into a minimum (stable critical point) and a maximum (unstable critical point). Since the double critical point splits into two critical points of different stability, it is a heterogeneous double critical point.

The investigation of the spinodal and the critical points give first indications how the binodal is built up. For three $\Delta\epsilon$-values the phase diagrams are shown in Figure 6. First the binodal is discussed for a value of $\Delta\epsilon$ where the two new critical points have just developed. As can be seen in Figure 6a there exists a new, additional binodal. This new binodal can be better seen in Figure 6b. It is the typical self-contained double-sigmoidal shape[4] when the unstable binodals emerge from a heterogeneous double critical point. The phase diagram is similar to that in Figure 8 of ref 4 where a detailed description can be found.

The second phase diagram (Figure 6c) for a lower value of $\Delta\epsilon$ is an example for the case that the new bisigmoidal binodal generated at the heterogeneous double critical point protrudes the envelope of the original binodal. The left minimum of the spinodal in Figure 6a now shifts out of the two-phase area of the original binodal and the minimum becomes a stable critical point as $\Delta\epsilon/k$ is changed from -0.06 to -0.08 K. The intersections of the S/S binodals fix the three coexisting phases. The region of that at the highest value of ϕ_1 is enlarged in Figure 6d. A more comprehensive discussion of a phase diagram like this is given in Figure 9 of ref 4.

Further decreasing $\Delta\epsilon$ leads to a change in the location of the bisigmoid as can be seen in Figure 6e. The two noncritical minima of the binodal at low ϕ_1 values in Figure 6c collapse, and two new cusps in Figure 6e are created. Simultaneously, the two cusps at the right-hand side fuse and split into two new noncritical extrema. This means the original stable critical point is now located on the bisigmoidal binodal, the bisigmoid is situated on the right-hand side of the phase diagram, and the pair of cusps at the left-hand side. A vanishing of the bisigmoid in a double critical point at the right-hand side which would bring the unstable binodals to an end in another double critical point is not realized by further decreasing $\Delta\epsilon$. The developments due to changing $\Delta\epsilon$ are very similar to those observed for changing interactions in a Flory−Huggins system.[4]

Polymers with Polar Interactions. The second example deals with a description[10] of the energy of mixing which distinguishes between two states of the mers, polar and nonpolar, originally introduced for a solution of poly(ethylene oxide) in water. The parameter P gives the probability that a segment is found in one of the polar states, and $(1 - P)$ is the probability for the nonpolar conformations. The basis is the Flory−Huggins theory[11] which is extended accounting for the multiple combinations of interacting segments; the interaction between solvent and the polar segment (χ_{12p}) is different from that of the solvent with the nonpolar segment (χ_{12u}). Two more pairs of interactions that contribute to the Gibbs energy are the interaction between polar and nonpolar segments (χ_{2p2u}) and between the nonpolar segments itself (χ_{2u2u}). In polar solvents P increases with the content of the solvent. The parameter F is given as the quotient of nonpolar and polar conformations and is set to 8 as in ref 10:

$$\overline{\overline{\Delta G}}/RT = \varphi_1\varphi_2[P\chi_{12p} + (1-P)\chi_{12u}] + \varphi_2^2\left\{(1-P)P\chi_{2p2u} + (1-P)^2\frac{\chi_{2u2u}}{2}\right\} + \varphi_1 \ln \varphi_1 + \frac{\varphi_2}{N_2}\ln \varphi_2 + \varphi_2\{P \ln P + (1-P)\ln[(1-P)/F]\} \quad (25)$$

For each composition, the value of P is determined in an iteration process using the condition

$$\overline{\overline{\Delta G}}(P) = \min \quad (26)$$

Since the Gibbs energy is only numerically accessible, the calculation of derivatives and so the chemical potentials is difficult, and the classical method for the calculation is not suitable.

The four interaction parameters are assumed to depend linearly on the inverse of the temperature according to

$$\chi_{ij} = \omega_{ij}/RT \quad (27)$$

Figure 7 shows such a phase diagram for a solution of a polar polymer with 100 segments per molecule ($N_2 = 100$). The Gibbs energy is given by eq 25 with the interaction parameters $\chi_{12p} = 5$ kJ mol$^{-1}/RT$, $\chi_{12u} = 7$ kJ kJ mol$^{-1}/RT$, $\chi_{2p2u} = 10$ kJ mol$^{-1}/RT$, and $\chi_{2u2u} = 11$ kJ mol$^{-1}/RT$. The insert gives the composition dependence of the fraction of polar segments P.

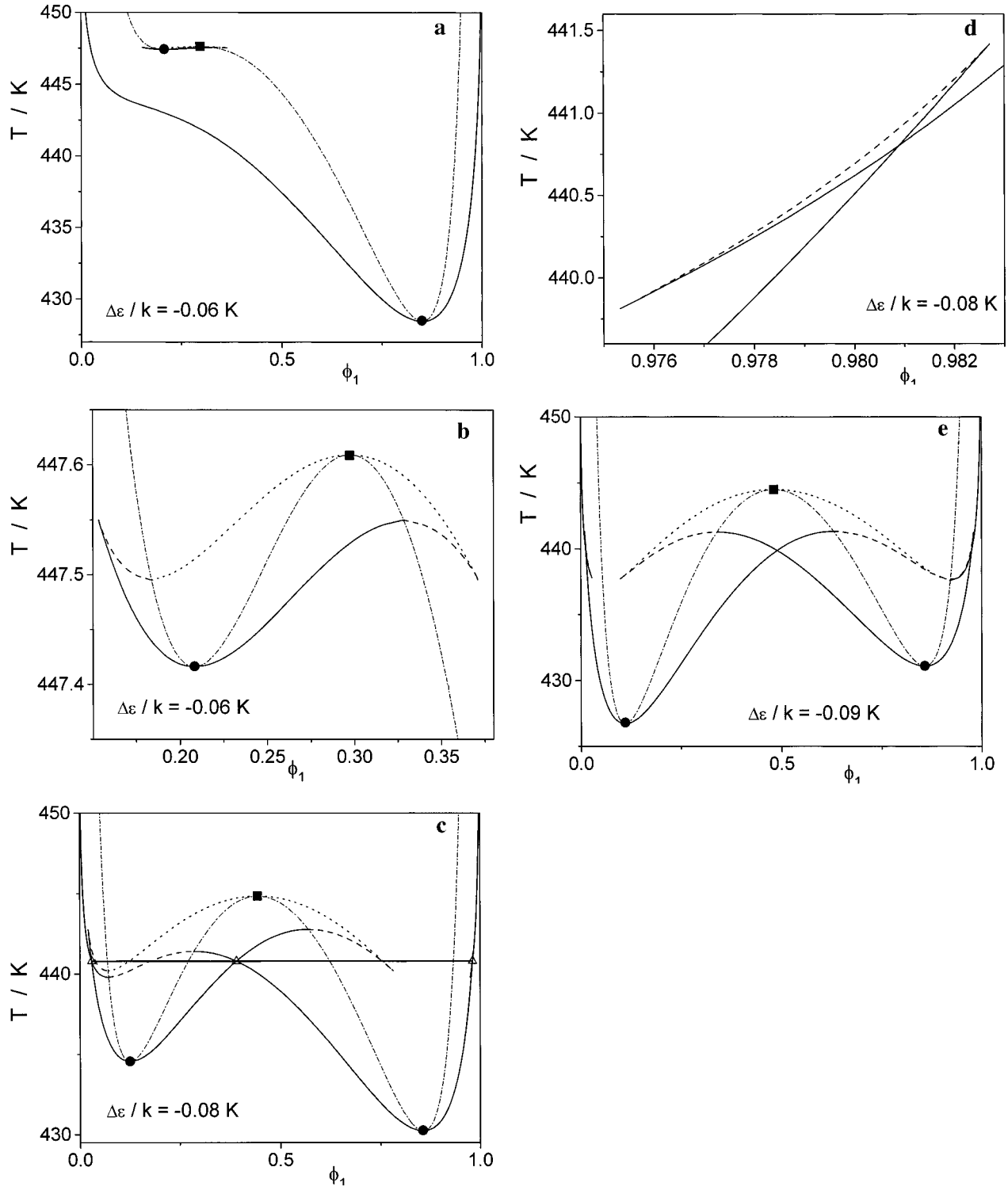

Figure 6. Phase diagrams for three values of $\Delta\epsilon$ given in the graph. Dash−dot line: spinodal, solid lines: S/S branches of the binodal, dotted line: U/U, dashed lines: U/S, open triangles and connecting solid line: three-phase equilibrium. Other symbols as in Figure 4.

This parameter decreases markedly with increasing temperature and decreasing φ_2.

The main region of immiscibility caused by the high value of χ_{12u} can be found at low φ_2 where the nonpolar segments of the polymer predominate. At high φ_2 and relatively low temperatures a second range of immiscibility is induced by the high content of polar segment, the interaction of which with the solvent is slightly better than that of the nonpolar mers. The phase diagram is similar to that of Figure 6e after a rotation by 180°.

Conclusion

The phenomena connected with the three-phase line and the phase rule are summarized in refs 2 and 12. Only the items concerning the binodal are mentioned here:

Three types of tie lines can be distinguished. All types fulfill the condition of equality of chemical potentials for each component.

The S/S tie lines refer to a minimum of the energy of mixing of the phase-separated system (stable: absolute minimum; meta-

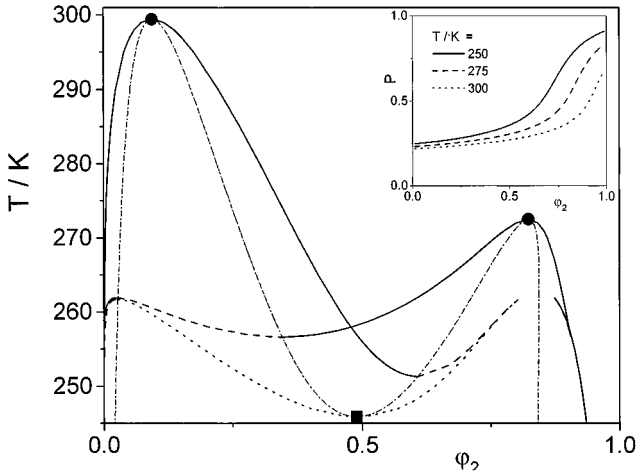

Figure 7. Phase diagram for a solution of a polar polymer with 100 segments/molecule. The Gibbs energy is given by eq 25 with the interaction parameters $\chi_{12p} = 5$ kJ mol^{-1}/*RT*, $\chi_{12u} = 7$ kJ kJ mol^{-1}/*RT*, $\chi_{2p2u} = 10$ kJ mol^{-1}/*RT*, and $\chi_{2u2u} = 11$ kJ mol^{-1}/*RT*. The insert gives the composition dependence of the fraction of polar segments. Symbols as in Figure 4, line types as in Figure 6.

stable: local minimum). Both end points are situated within the (meta)stable area of the phase diagram. The stable parts of the binodal separate the one-phase from the two-phase regions. The S/S branches of the binodal change from metastable to stable at the three-phase line. A (meta)stable critical point is located on a S/S binodal.

The U/U tie lines refer to a maximum of the energy of mixing; both nodes are within the unstable area. An unstable critical point is located on a U/U binodal.

The U/S tie lines are related with a saddle point of the energy of mixing. One node is situated within the unstable region, one within the metastable area.

The S/S meet the U/S binodals at a cusp within the metastable area or at the corresponding noncritical extremum.[4] The U/U meet the U/S binodals at a cusp within the unstable area or at the corresponding noncritical extremum. The S/S and U/U binodals never meet.

Acknowledgment. I would like to thank Prof. R. Koningsveld for drawing my attention to the phenomenon of unstable binodals. The support of the Deutsche Forschungsgemeinschaft, DFG-Schwerpunkt "Stoffeigenschaften komplexer fluider Gemische", is gratefully acknowledged.

References and Notes

(1) Korteweg, D. J. *Sitzungsberichte der kais. Akad. d. Wiss. math.-naturw. Classe XCVIII. Abth. II. a*; Wien, 1889; p 1154.
(2) van der Waals, J. D.; Kohnstamm, Ph. *Lehrbuch der Thermostatik;* Leipzig, 1927.
(3) Tompa, H. *Polymer Solutions*; Butterworth Scientific Publications: London, 1956
(4) Šolc, K.; Kleintjens, L. A.; Koningsveld, R. *Macromolecules* **1984**, *17*, 573.
(5) Šolc, K.; Koningsveld, R. *J. Phys. Chem.* **1992**, *96*, 4056.
(6) Horst, R. *Macromol. Theory Simul.* **1995**, *4*, 449; **1996**, *5*, 789.
(7) Guffey, C. G.; Wehe, A. H. *AIChE J.* **1972**, *18*, 913.
(8) Sanchez, I. C.; Lacombe, R. H. *J. Phys. Chem.* **1976**, *80*, 2352, 2568.
(9) Sanchez, I. C.; Balasz, A. C. *Macromolecules* **1989**, *22*, 2325.
(10) Karlström, G. *J. Phys. Chem.* **1985**, *89*, 4962.
(11) Flory, P. J. *Principles of Polymer Chemistry*; Cornell University Press: Ithaca, NY, 1953.
(12) Koningsveld, R.; Berghmans, H.; Nies, E. *Prog. Colloid Polym. Sci.* **1994**, *96*, 46